Geophys. J. R. astr. Soc. (1979) **57**, 507–534

Observational constraints on the chemical and thermal structure of the Earth's deep interior

Guy Masters *Department of Geodesy and Geophysics, University of Cambridge*

Received 1978 November 10; in original form 1978 July 13

Summary. The observations of the periods of free oscillation of the Earth provide direct constraints on the density distribution in the Earth. These in turn allow constraints to be placed on the size of departures from a state of adiabaticity and chemical homogeneity. These departures are quantified in terms of a stratification parameter 'η' first introduced as an index of chemical homogeneity. The resolving power theory of Backus & Gilbert is used to determine the ability of the observed free oscillations to constrain η in the lower mantle and outer core. The results suggest that the outer core is not strongly chemically stratified although a significantly thermally stable core cannot be excluded. The free oscillations also apparently require a compositional difference between the inner and outer cores.

1 Introduction

It has recently been shown that the lower mantle and core of the Earth can have a density distribution consistent with that of an adiabatic and homogeneous region. This important result has been established by Dziewonski, Hales & Lapwood (1975) whose earth model, PEMA, closely follows the Adams–Williamson relation in these regions. This model apparently gives a satisfactory fit to a large amount of seismological data including the periods of a large number of normal modes. The question remains as to how well these data constrain the density distribution. For example, can the lower mantle or core be significantly thermally or chemically stratified and still be consistent with these data? How detailed is the structure we can resolve? These and other questions can be answered using linear resolving power theory (Backus & Gilbert 1968, 1970) providing certain conditions are satisfied, notably that the models of the Earth are linearly close to the real Earth.

The measure of 'stratification' used in this study is a measure of the departure of a region from the 'reference' state of adiabaticity and homogeneity. The density gradient in an adiabatic and homogeneous region in hydrostatic equilibrium is given by the well-known Adams–Williamson relation

$$\frac{d\rho}{dr} = -\frac{g\rho}{\phi} \tag{1.1}$$

where g is the acceleration due to gravity, ρ is the density and ϕ is the seismic parameter given by

$$\phi = \frac{K_s}{\rho} = V_p^2 - \frac{4}{3} V_s^2. \tag{1.2}$$

K_s is the adiabatic bulk modulus and V_p, V_s are the compressional and shear wave velocities respectively. A useful measure of departure from this state was given by Bullen (1963):

$$\eta = -\frac{\phi}{\rho g} \frac{d\rho}{dr} \tag{1.3}$$

or equivalently

$$\eta = \frac{dK_s}{dp} + \frac{1}{g} \frac{d\phi}{dr} \tag{1.4}$$

where p is the pressure and $dK_s/dp \equiv (dK_s/dr)/(dp/dr)$. Bullen used this measure to infer departures from homogeneity by arguing that dK_s/dp is slowly varying in the Earth and using values of $d\phi/dr$ derived from travel-time data (see Bullen 1975 for a review). A difficulty with this early approach is the unknown precision of the velocity gradients used to calculate $d\phi/dr$. If the main contributor to the uncertainty of η is the uncertainty in $d\phi/dr$ then resolving power theory could be used to constrain the velocity gradients (Johnson & Gilbert 1972) and so determine the possible variable in η. While it is reasonable to suppose that dK_s/dp is slowly varying in regions which are near adiabaticity there is no compelling reason to believe this to be true in a region of high temperature gradient. Indeed $|1/K_s(\partial K_s/\partial T)_p|$ is of the order of three to five times larger than the coefficient of thermal expansion (Birch 1952) and in a thermal boundary layer this could give a significant reduction in dK_s/dp. For this reason free oscillation data have been used to directly investigate η as defined by equation (1.3). This definition is stressed because η has been interpreted solely as an index of chemical inhomogeneity whereas (1.3) implicitly has a contribution from non-adiabatic temperature variations (Bullen 1967). A common alternative measure of stratification was introduced by Pekeris & Accad (1972) which they called β where

$$\beta = 1 + \frac{\phi}{\rho g} \frac{d\rho}{dr} \tag{1.5}$$

so that

$$\beta = 1 - \eta. \tag{1.6}$$

Yet another measure in a fluid is the Brunt–Vaisäla frequency, N which is related to η by

$$N^2 = \frac{g^2}{\phi}(\eta - 1). \tag{1.7}$$

While the Brunt–Vaisäla frequency has a more obvious physical significance (see below), (1.3) is preferred in the present context for reasons of algebraic simplicity.

Fig. 1 shows η as a function of radius in the Earth calculated for three recent earth models, 1066 A and B of Gilbert & Dziewonski (1975) and PEMA of Dziewonski *et al.* (1975). These three models have been constructed using all the available normal mode data and it is immediately clear that the dataset does not constrain η at all well in the inner core and upper mantle. The poor ability of the modes to resolve upper mantle structure has been

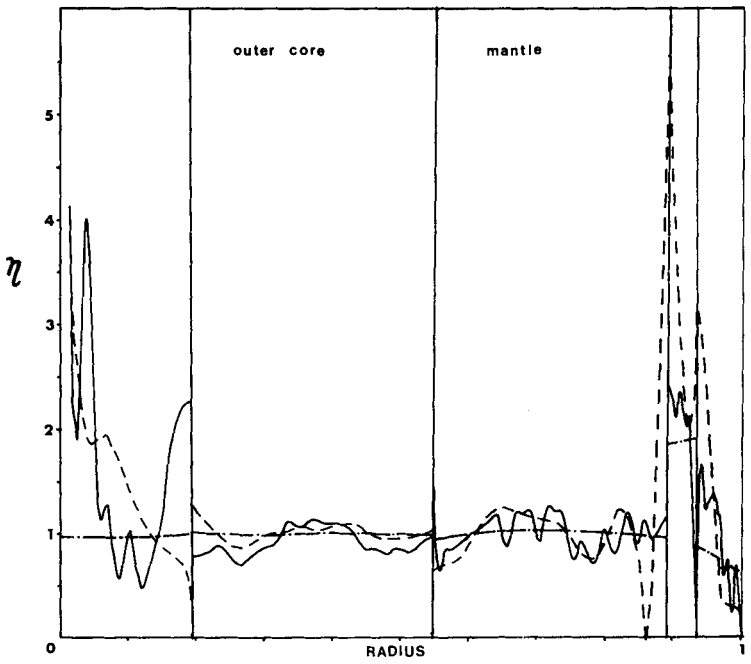

Figure 1. The stratification parameter, η, as a function of radius for three recent earth models – 1066A (broken line), 1066B (solid line) and PEMA (chain dotted line).

discussed by Dziewonski *et al.* (1975) who also conclude that no detectable bias is introduced by the choice of upper mantle model. We therefore concentrate our attention on the lower mantle and outer core. η is a measure of the ability of a region to convect and it is therefore of particular relevance to the geodynamo if the core can be significantly thermally or chemically stratified. A related parameter is the density jump at the inner core boundary (ICB). This has varied considerably in recent earth models from $0.2 \rightarrow 0.9$ Mg m^{-3} and it is not clear if the normal mode data even require its presence. Proof of its existence has implications for the composition of the inner core and consequently for the power source of the geodynamo (Gubbins 1977). For these reasons it has been considered in detail in this paper although the method used applies to any parameter discontinuity and gives a simple way to determine the resolvability of such features provided the relevant Fréchet derivatives exist. In most other respects recent models of the deep Earth are in remarkable agreement and it is felt that an investigation into the reasons for the more obvious disagreements is now justified.

2 Thermodynamic and hydrodynamic aspects of stratification

Consider a mixture of n components with each component labelled by the subscript i. If the specific entropy s, is regarded as a function of temperature, pressure and composition, its radial gradient may be expressed as:

$$\frac{ds}{dr} = \alpha g + \frac{C_p}{T}\frac{dT}{dr} + \sum_{i=1}^{n}\left(\frac{\partial s}{\partial x_i}\right)_{p,\,T,\,x_j}\frac{dx_i}{dr} \tag{2.1}$$

α, C_p, T and x_i are the coefficient of volume expansion, specific heat, temperature and a measure of the amount of component i respectively. The adiabatic temperature gradient is obtained by setting $ds/dr = 0$:

$$\left(\frac{dT}{dr}\right)_s = -\frac{gT\alpha}{C_p} - \frac{T}{C_p}\sum_{i=1}^{n}\left(\frac{\partial s}{\partial x_i}\right)_{p,\,T,\,x_j}\frac{dx_i}{dr}. \tag{2.2}$$

Defining the actual temperature gradient (by analogy with Birch 1952)

$$\frac{dT}{dr} = \left(\frac{dT}{dr}\right)_s - \tau \tag{2.3}$$

we can write the expression for the radial gradient of density:

$$\frac{d\rho}{dr} = -\frac{g\rho}{\phi} + \alpha\rho\tau + \sum_{i=1}^{n}\left(\frac{\partial\rho}{\partial x_i}\right)_{p,\,s,\,x_j}\frac{dx_i}{dr}. \tag{2.4}$$

Using equation (1.3), η can be written:

$$\eta = 1 - \frac{\alpha\phi\tau}{g} - \frac{\phi}{\rho g}\sum_{i=1}^{n}\left(\frac{\partial\rho}{\partial x_i}\right)_{p,\,s,\,x_j}\frac{dx_i}{dr}. \tag{2.5}$$

(2.5) clearly shows the separate contributions of departures from adiabaticity and departures from homogeneity. We refer to η as the stratification parameter as it is a measure of how much a region is chemically or thermally stratified. The physical significance of η can be demonstrated by the following argument. Consider a small radial displacement of a parcel of material. Let us suppose that this displacement is rapid compared to the diffusion times of heat and matter in the locality. The parcel will then move with constant entropy and composition and, for a displacement Δ, will have a new density, ρ_p given by:

$$\rho_p = -\frac{g_0\rho_0}{\phi_0}\Delta + \rho_0. \tag{2.6}$$

The subscript zero refers to the initial state before displacement. The ambient material will have a density

$$\rho_a = -\frac{g_0\rho_0}{\phi_0}\Delta + \alpha_0\rho_0\tau\Delta + \sum_{i=1}^{n}\left(\frac{\partial\rho}{\partial x_i}\right)_{p,\,s,\,x_j}\frac{dx_i}{dr}\Delta + \rho_0. \tag{2.7}$$

The density difference between the parcel and its surroundings is:

$$\rho_a - \rho_p = \alpha_0\rho_0\tau\Delta + \sum_{i=1}^{n}\left(\frac{\partial\rho}{\partial x_i}\right)_{p,\,s,\,x_j}\frac{dx_i}{dr}\Delta. \tag{2.8}$$

If we neglect viscous, rotational and magnetic effects then it follows that, for a positive radial displacement, the parcel is buoyant if $\rho_p < \rho_a$. The buoyancy forces on the parcel will cause it to continue to move so giving convection. Conversely, if $\rho_p > \rho_a$ then the parcel will return to its original position and convection is inhibited. If convection is to occur then inspection of (2.8) shows that

$$\tau \geqslant -\frac{1}{\alpha\rho}\sum_{i=1}^{n}\left(\frac{\partial\rho}{\partial x_i}\right)_{p,s,x_j}\frac{dx_i}{dr} \tag{2.9}$$

or

$$\eta \leqslant 1. \tag{2.10}$$

A stable region in which convection cannot occur is characterized by $\eta > 1$. The condition $\eta = 1$ corresponds to neutral stability. If $\eta > 1$ then a displacement of a parcel of fluid leads to an oscillation with a frequency given by the Brunt–Vaisäla frequency, N. When $\eta < 1$, N is interpreted as the exponential growth rate of the instability. Note that N is useful only for a fluid. If we take into account the viscous, rotational and magnetic effects then η must be less than one before convection will occur. It is possible to estimate just how small η must be before instability sets in. Consider, first, the lower mantle; this region is represented as a Newtonian fluid with constant viscosity for the purpose of this estimate. Rotational effects are negligible because of the large viscosity so the Rayleigh number can be written in the form $\alpha g \tau d^4/\kappa\nu$ where d is a characteristic scale length, κ is the thermal diffusivity and ν is the kinematic viscosity. The critical Rayleigh number for a plane layer is $0(10^3)$, the exact value depending upon the boundary conditions of the convecting region. A similar value is appropriate for a spherical shell of thickness $a/2$, where a is the external radius, with free surfaces (Chandrasekhar 1961). This allows us to estimate τ_c the critical superadiabatic gradient which gives η_c, the value of η at the onset of convection. Assuming homogeneity (2.5) gives:

$$\eta_c = 1 - \frac{\alpha\phi\tau_c}{g} = 1 - \frac{\phi\kappa\nu 10^3}{g^2 d^4}.$$

We adopt the following values appropriate for the lower mantle:

$$g = 10\ \mathrm{m^2 s^{-1}}, \quad \kappa = 10^{-6}\mathrm{m^2 s^{-1}}, \quad d = 2 \times 10^6\mathrm{m}, \quad \phi = 10^8\mathrm{m^2 s^{-2}}, \quad \nu = 10^{17}\text{–}10^{22}\mathrm{m^2 s^{-1}}.$$

The large uncertainty in ν leads to the following range of values for η_c

$$0.4 < \eta_c < 0.999994.$$

The smaller value is associated with the higher viscosity suggested by Mckenzie (1966). This value corresponds to a superadiabatic gradient of about 3 K/km. If the amount of heat from the core plus the internal heat in the lower mantle is too great to be removed by conduction then superadiabatic gradients will be formed. However it is anticipated that the temperature rise due to these effects will lower the viscosity so that $\eta_c \to 1$ (Tozer 1972) long before an η of 0.4 is established. If the kinematic viscosity is less than $10^{20}\mathrm{m^2 s^{-1}}$ as suggested by Goldreich & Toomre (1969) then η_c is insignificantly less than one as far as the seismic observations are concerned. If the lower mantle convects then numerical experiments have shown that the bulk of the convecting region is adiabatic (Jarvis, private communication). Boundary layers develop depending upon the mode of heating. If the heating is dominantly internal then there will be no thermal boundary layer at the base of the mantle. If there is substantial heat flux from the core than a boundary layer will exist at the bottom. Numerical calculations by Mckenzie, Roberts & Weiss (1974) show that, in a Boussinesq fluid, the boundary layer occupies about 1/10 of the layer thickness; this result depends only weakly on the heat flux through the boundary and has also been verified for simple non-Boussinesq materials (Jarvis, private communication). We might therefore expect a strong superadiabatic gradient at the base of the mantle occupying a region up to 200 km thick. This region also shows peculiarities in elastic structure; for a review see Jacobs (1975) and Cleary (1974). These have been interpreted in two different ways. Bolt (1972) infers an abnormal increase in density in this region which could be caused by the advection of core material into the lower mantle (presumably at a time when the lower mantle was nearer its

melting point). This interpretation leads to an estimated η of about 4.9 using Bolt's determination of the seismic velocity gradients. Jones (1977) has considered the alternative interpretation of a thermal boundary layer and, again using Bolt's velocity gradients, estimates a temperature gradient of about 12 K/km, this corresponds to an η of -1.7 if the region is homogeneous. It is clearly important to distinguish between these cases.

Summarizing the possibilities we have:

(1) η significantly greater than one in the bulk of the lower mantle. This implies chemical inhomogeneity or sub-adiabatic temperature gradient.

(2) $\eta \simeq 1$ throughout the lower mantle. This implies a convecting mantle. If the base of the mantle is characterized by $\eta \simeq 1$ then the heating is dominantly internal, if η is significantly less than one then there is a substantial heat flux from the core.

(3) η significantly less than one. This implies a high viscosity with strong superadiabatic temperature gradients.

Consider now the outer core. The low viscosity of this region (Gubbins 1976) implies that such a large body will require only very small superadiabatic gradients or compositional gradients to initiate convection. To see this we consider the following argument. Suppose a superadiabatic gradient exists in the core such that there is a convected heat flux equivalent to 10^{13}W out of the surface of the core (this large value is used for the purpose of illustration). The convected heat flux per square metre per second is given by

$$q = \rho v_r C_p \tau \Delta \tag{2.11}$$

where v_r is the average radial convective velocity and Δ is a characteristic length scale of the convective displacement. In a homogeneous core η is given by

$$\eta = 1 - \frac{\alpha \phi \tau}{g} = 1 - \frac{\gamma q}{\rho g v_r \Delta} = 1 - \delta$$

where γ is the thermodynamic Grüneisen ratio defined by $\gamma = \alpha K_s / \rho C_p$. If core convection is large scale with velocities similar to those inferred from the westward drift of the geomagnetic field then $v_r \Delta \simeq 100$ and $\delta = 5 \times 10^{-9}$. Even for this very large convected heat flux δ is tiny so that at the onset of convection it is reasonable to suppose that η is insignificantly less than one. If core motions are dominated by rotation then Busse (1975) shows that a much smaller length scale of convection is appropriate although the velocities are larger. Busse's work leads to a critical superadiabatic gradient of 3×10^{-6} K/m which gives an η of 0.9998 at the onset of convection. Once the outer core convects the temperature will be distributed adiabatically and the core will be well mixed (Gubbins & Masters, in preparation). Thermal boundary layers may develop but, in the case of the outer core, will be too thin to resolve using normal mode data. Summarizing, η will appear to be one if the core is convecting and will be greater than one if subadiabatic temperature gradients exist or if there is inhomogeneity. It is very unlikely that η will be significantly less than one in this region. We can estimate how large η can become if the core is stable. First consider a homogeneous subadiabatic core. The most stable the core could reasonably become is isothermal, then η becomes

$$\eta_{iso} = 1 + \alpha T \gamma = 1.04.$$

Higgins & Kennedy (1971) suggested that the core was subadiabatic with a temperature difference across the region of about 500 K. This gives an η of ~ 1.03. This is a relatively small increase and in fact η is much more sensitive to variations in chemical composition, a point noted by Bullen. To illustrate this, consider an adiabatic inhomogeneous core. η

may be written

$$\eta = 1 - \frac{\phi}{\rho g} \sum_{i=1}^{n} \left(\frac{\partial \rho}{\partial x_i}\right)_{p,\, T,\, x_j} \frac{dx_i}{dr} - \frac{\gamma}{g} \sum_{i=1}^{n} Q_i \frac{dx_i}{dr} \tag{2.12}$$

where

$$Q_i = T\left(\frac{\partial s}{\partial x_i}\right)_{p,\, T,\, x_j}.$$

Q_i is the heat of reaction. For the purpose of our estimate consider the core as a simple binary mixture of iron plus an impurity such as sulphur or silicon. Gubbins (1977) has given estimates of Q and $(\partial\rho/\partial x)_{p,\,T}$ may be estimated assuming the mixture is ideal. Usselman (1975) suggests that x is about 10 per cent if sulphur is the impurity with a likely variation of 3 per cent across the outer core. Because $\phi/\rho g$ varies by a factor of 3 across the region, η varies from 1.23 at the ICB to 1.07 at the MCB (if a uniform compositional gradient is assumed) with an average value of 1.13. One goal of this work is to see if the data allow such compositional changes. A final point to note is that, because of the variation of ϕ and g in the outer core, η is more sensitive to departures from homogeneity and adiabaticity near the ICB.

3 The normal mode dataset

The dataset used in this study is a subset of the 1064 observed normal mode frequencies presented by Gilbert & Dziewonski (1975). To some extent both the observed frequencies and their assigned errors have been derived using model-dependent procedures. Where more than one observation of a mode was available the authors chose, as a 'best' value, the frequency closest in a least-squares sense to the frequencies predicted for that mode by models 1066A and B. The procedures used to identify modes give no clear indication of the error on the observation and various qualitative measures were used to initially assign the errors. These errors were then adjusted so that the residuals of 1066A and B were normally distributed. The residuals do in fact show little bias suggesting that systematic errors in the observations are small, although these may account for a few very badly fitted modes. The international deployment of long period accelerometers (Project Ida – Berger, Agnew & Farrell 1975) has meant that a large amount of high-quality long-period data is becoming available. This should do much to alleviate the problems in the existing dataset. Assuming that the errors and observations have been correctly assigned then inspection of the distribution of residuals will tell us if a model 'fits' the data. The errors are assumed to be normally distributed with zero mean and so we can expect no more of a model if its residuals show a similar distribution. 1066A does exhibit a good distribution of residuals in this respect, with some exceptions, but 1066B has a non-zero mean of one-third of a standard deviation which, as Gilbert & Dziewonski (1975) noted, implies that 1066B could be iterated further. For comparison, the distribution of residuals for model PEM-A of Dziewonski *et al.* (1975) is shown in Fig. 2. With the errors assigned using 1066A and B these residuals are not normally distributed and the errors on the modes would have to be made larger still to achieve this. If the errors have been correctly assigned we can say that 1066A is a better fit to the data than PEM-A which is hardly surprising in view of the parametric simplicity of PEMA. It would be premature, in view of the above comments, to infer that PEMA is too simply parameterized to give a 'good' fit to the data. Some modes are badly fitted by individual models but the same modes are not badly fitted by all models. This makes it

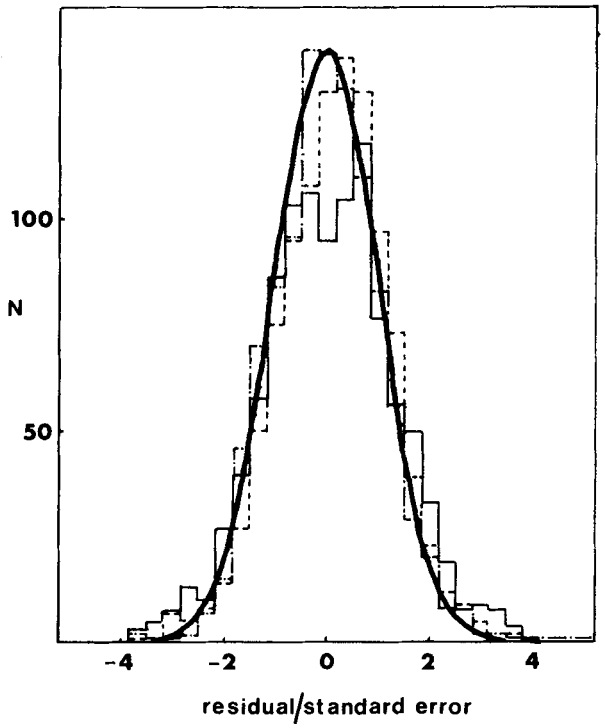

Figure 2. Histograms of relative residuals of the observed eigenfrequencies computed for 1066A (chain dotted line), 1066B (broken line) and PEMA (solid line). The heavy line is the error curve for the normal distribution.

difficult to identify modes contaminated with systematic error of some sort. An interesting case is the mode ${}_{11}S_2$ which was used by Dziewonski & Gilbert (1973) as direct evidence for the solidity of the inner core. 1066A gives a very bad fit to this mode (18 standard deviations), however, one cannot immediately infer that the mode has been misidentified particularly in view of the careful analysis of Dziewonski & Gilbert. 1066B, which has a slightly lower inner core shear velocity and smaller inner core radius than 1066A, gives a good fit to ${}_{11}S_2$ but apparently at the expense of other modes which strongly sample this region. For example ${}_{10}S_2$, ${}_{13}S_5$, ${}_{18}S_6$ and ${}_{20}S_9$ are all much worse fitted in 1066B than in 1066A. It should also be noted that ${}_{10}S_2$ and ${}_{11}S_2$ change their mode characteristics from 1066A to 1066B and it is ${}_{10}S_2$ which strongly samples shear energy in the inner core in 1066B. This discussion serves to illustrate the complex tradeoffs involved between shear velocity and radius of the inner core and a separate investigation has been undertaken to see if there is a model which will give a satisfactory fit to all these data. In the interim, 1066A gives the best fit to the data from our point of view and has been used as a reference model in the resolving power calculations.

The subset of modes used in the calculations consisted of the 400 observed spheroidal modes with the smallest angular order number. This was the largest dataset that could be conveniently handled on the Cambridge computer. All modes with significant energy in the core are included, this is the region of primary interest in this study. There are about 260 remaining observed spheroidal overtones of high angular order ($l > 30$) many of which have similar displacements to modes in the restricted dataset. The loss of information incurred by the removal of these and the toroidal modes is small and is largely confined to the upper

mantle. Because of the above comments no modes were culled from the dataset but the data were ranked and winnowed following the method described by Gilbert (1971). A pronounced condensation of small eigenvalues was noted making the cutoff point between 'significant' and 'insignificant' recombinations of the data difficult to determine. The first 150 recombined data were retained for further study. The Fréchet kernels for the modes were computed from eigenfunctions calculated for model 1066A. These were generously provided by Dr R. Buland and Professor F. Gilbert.

4 The determination of significant features of stratification

Using Rayleigh's principle, Backus & Gilbert (1967) have derived an expression relating the perturbations in the radial distribution of density, bulk modulus and rigidity to the perturbation of the eigenfrequency of a normal mode of an SNREI (spherical, non-rotating, elastic, isotropic) earth. Their equation (49) can be rewritten in terms of relative perturbations in seismic velocities and densities so that, for an individual mode, we have

$$\frac{\delta\omega}{\omega} = \int_0^1 \left(K_{v_p} \frac{\delta v_p}{v_p} + K_{v_s} \frac{\delta v_s}{v_s} + K\rho \frac{\delta\rho}{\rho} \right) r^2 \, dr \tag{4.1}$$

where the Ks are simple functions of the eigenfunctions of the mode (Backus & Gilbert 1967). If internal discontinuities in elastic parameters are also perturbed then there are additional terms in the above equation (Woodhouse 1976). This possibility will not be considered further here.

The stratification parameter, η, can be calculated from a knowledge of ρ, v_p and v_s and, in principle, an estimate of the uncertainty in this determination can be made using the uncertainties in the individual seismic parameters. It is difficult to estimate the uncertainty in the density gradient and it is obviously much more convenient to reformulate the problem with η replacing one of the model parameters ρ or v_p. The natural choice is to replace ρ so that the problem is reformulated in terms of η, v_p and v_s. The reason for this is that the velocities are better determined than the density and this reformulation allows us to localize information about the stratification much better in the resolving power analysis (see below). Equation (4.1) becomes:

$$\frac{\delta\omega}{\omega} = \fint_0^1 \left(\kappa_\eta \frac{\delta\eta}{\eta} + \kappa_{v_p} \frac{\delta v_p}{v_p} + \kappa_{v_s} \frac{\delta v_s}{v_s} \right) dr + \sum_{k=1}^{n} A_k \left[\left(\frac{\delta\rho}{\rho} \right)^+_- \right]_k . \tag{4.2}$$

The sum k is taken over all discontinuities and $[\delta\rho/\rho]^+_-$ signifies the difference in perturbation in density on either side of a discontinuity. The sign $\fint$ means integration over regions between discontinuities but not through the discontinuities themselves. These minor complications arise because of the singularity in η at a density discontinuity. Without information about the change in density at a discontinuity, the density distribution could not be retrieved uniquely from the radial distribution of stratification, this information is provided by the last term in (4.2). Expressions for the kernels in (4.2) are given in Appendix A. The comments of the previous section might lead us to believe that $\eta \simeq 1$ in large parts of the lower mantle and outer core. Equation (4.2) clearly allows us to perturb an earth model while retaining this feature. PEMA of Dziewonski *et al.* (1975) is such a model (Fig. 1) which indicates that it is possible to achieve a 'satisfactory' fit to a large amount of data with the constraint that $\eta = 1$ in most of the deep Earth. Our main interest is to determine how large perturbations from this state can be. This is a straightforward application of resolving power theory (Backus & Gilbert 1968, 1970).

For reasons discussed in the previous section model 1066A is used as a reference model and this is assumed to be linearly close to the real Earth. Modern earth models are sufficiently similar in the lower mantle and outer core to conclude that this assumption is probably valid in these regions. The $\partial\omega/\omega$ in equation (4.2) is interpreted as the relative difference between the observed period of a mode and the period calculated for 1066A. (In fact we use the 'significant' recombination of these residuals given by the ranking and winnowing procedure but the principle is the same.) A linear combination of the data is taken

$$\sum_{i=1}^{m} a_i \frac{\delta\omega_i}{\omega_i} = \int_0^1 \left(R_\eta \frac{\delta\eta}{\eta} + R_{v_p} \frac{\delta v_p}{v_p} + R_{v_s} \frac{\delta v_s}{v_s} \right) dr + \sum_{k=1}^{n} R_k \left[\left(\frac{\delta\rho}{\rho} \right)^+ \right]_k \tag{4.3}$$

where m is the number of data and n is the number of density discontinuities and

$$R_\eta = \sum_{i=1}^{m} a_i \kappa_{\eta_i}(r)$$

with similar expressions for the other Rs.

The a_is are chosen to fulfil a specific task. If we wish to determine the stratification parameter at a radius r_0 in the Earth we choose the a_is to fulfil as nearly as possible:

$$R_\eta = \delta(r - r_0)$$

and

$$R_{v_p} = R_{v_s} = R_k = 0.$$

This is achieved by minimizing the quadratic form:

$$S = \sum_{ij} a_i a_j S_{ij}$$

$$S_{ij} = 12 \int_0^1 (r - r_0)^2 \kappa_{\eta_i} \kappa_{\eta_i} \, dr + \int_0^1 \lambda_{v_p}(r) \; \kappa v_{p_i} \kappa_{v_{pj}} \, dr + \int_0^1 \lambda_{v_s}(r) \; \kappa_{v_{si}} \kappa_{v_{ij}} \, dr \tag{4.4}$$

$$+ \sum_{k=1}^{n} A_{ik} A_{jk} \lambda_k$$

subject to the side constraint

$$\sum_{i=1}^{m} a_i \int_0^1 \kappa_{\eta_i} \, dr = 1.$$

The λs are arbitrary weightings which are discussed below. This definition of the 'spread', S, is similar to that introduced by Backus & Gilbert (1968, 1970). When S is minimized it is clear that R_η will have a peak near r_0, the width of this peak and its displacement from r_0 give a measure of our ability to resolve η at r_0. The factor 12 in (4.4) is introduced to make S a rough measure of the peak width (Backus & Gilbert 1970). If we had an infinite amount of accurate data then we could perform the minimization perfectly giving

$$\frac{\delta\eta}{\eta}(r_0) = \sum_{i=1}^{m} a_i \frac{\delta\omega_i}{\omega_i}. \tag{4.5}$$

Because we have a finite amount of data, Backus & Gilbert (1968) show that we can only find a local average of $\partial\eta/\eta$ over a resolving length. The inaccuracy in the data lead to an

error in the local average which is estimated by

$$\varepsilon = \left[\sum_{ij} a_i a_j E_{ij}\right]^{1/2} \tag{4.6}$$

where E_{ij} is the covariance matrix of the data. Backus & Gilbert (1970) show that it is impossible to minimize this error and the 'spread' simultaneously. The tradeoff between spread and error is calculated in the usual way by choosing the a_is to minimize M where

$$M = \sum_{ij} a_i a_j [S_{ij} \cos\theta + wE_{ij} \sin\theta] \qquad 0 \leqslant \theta \leqslant \pi/2.$$

θ is the tradeoff parameter and w is a weighting factor chosen to centre the calculation of the tradeoff curve about the knee.

It should be noted at this point that the choice of S_{ij} is largely arbitrary as long as a minimization of S leads to a resolving kernel of the desired shape. This may not even be peaked, for example, if we desire an estimate of the average stratification over some large region; the appropriate shape of resolving kernel is a boxcar over this region and the definition of S can be changed in an obvious way to fulfil this. Having said this, the definition (4.4) has the merit of giving a peaked resolving kernel with small side lobes which eases the interpretation of the results.

A small digression is now required to discuss an ambiguity which arises in linearized resolving power analysis. Suppose the reference model fitted the data exactly. Then, if this model is linearly close to the real Earth, Backus & Gilbert (1970) show that the local average over the resolving kernel is the same for the real Earth as the model, i.e. $\partial\eta/\eta(r_0) = 0$. Of course, no model will fit the data exactly, nor should it because of the errors in the observations. In this case

$$\sum_{i=1}^{m} a_i \delta\omega_i/\omega_i$$

will be non-zero (this is called the 'misfit' in what follows). The discussion of the previous section indicates that there is no point in continuing a fitting procedure once a model exhibits normally distributed residuals with zero mean (assuming the observational errors are uncorrelated). If a model fulfilled this exactly then a linear combination of residuals would have an expected value of zero and once again the local average over the model and the real Earth would be the same. 1066A was chosen as a reference model because its distribution of residuals was closest to this expected distribution. However, if the misfit is calculated using the residuals of 1066A, it is not particularly small. This is due mainly to several badly fitted modes (such as ${}_{11}S_2$). One approach would be to delete these modes from the original dataset to make the distribution of residuals 'normal' although arguments against this have been given above. If we admit the possibility that the badly fitted modes are telling us about a deficiency in our reference model and retain the belief that our model is linearly close to the real Earth then the misfit should be regarded as a correction to the local average over the model. In retrospect this is a little unreasonable as badly fitted modes will be due either to misidentification in which case they should be deleted or non-linearities of the nature described in the previous section. The calculations given below have assumed that the misfit has the expected value of zero. To simplify interpretation the following calculation is performed:

$$\sum_{i=1}^{m} a_i \left(\frac{\delta\omega}{\omega}\right)_i = \int_0^1 \frac{R_\eta}{\eta_m} \eta_e \, dr - \int_0^1 \frac{R_\eta}{\eta_m} \eta_m \, dr + C_{v_p} + C_{v_s} + C_\Delta \tag{4.7}$$

where

$$C_{v_p} = \int_0^1 R_{v_p} \frac{\delta_{v_p}}{v_p} \, dr$$

with similar obvious definitions of C_{v_s} and C_Δ. The side constraint used is

$$\int_0^1 \frac{R_\eta}{\eta_m} \, dr = 1$$

where η_m is the model value of η for model 1066A. The ith relative residual is given by

$$\left(\frac{\delta\omega}{\omega}\right)_i = \frac{\omega_{ei} - \omega_{mi}}{\omega_{mi}}.$$

The subscript m indicates the frequency calculated for model 1066A and the subscript e refers to the observed frequency. C_{v_p}, C_{v_s} and C_Δ compose what I have called the 'contamination' in the answer and is estimated below. Defining $R'_\eta = R_\eta/\eta_m$ we have, in the absence of contamination or significant misfit, a local average:

$$\bar{\eta}(r_0) = \int_0^1 R'_\eta \eta_e \, dr = \int_0^1 R'_\eta \eta_m \, dr. \tag{4.8}$$

The contamination contributes to the uncertainty on this local average along with the observational error given by (4.6). The contamination arises because we cannot perfectly remove the effect of the velocity distribution and density discontinuities. This has been bounded using

$$C_{v_p} \leqslant \int_0^1 |R_{v_p}| \left|\frac{\delta v_p}{v_p}\right|_{\max} dr$$

with similar expressions for the other contributions, C_{v_s} and C_Δ. $|\partial v_p/v_p|_{\max}$ is an *'a priori'* estimate of the maximum perturbation we expect from our model velocity. These *a priori* uncertainties are discussed in some detail in Appendix B and are summarized in Fig. 3. The bound on C_{v_p}, C_{v_s} and C_Δ is correct if the real Earth lies somewhere in the corridors shown in Fig. 3. These bounds may be very pessimistic. It would be possible to *estimate* contamination if we were prepared to make some assumption about the nature of the perturbation of the velocity about 1066A. For example, we could assume that the perturbations are random variables with zero mean and finite variance. This is probably inappropriate. Certainly, we do not expect that the real Earth will have a velocity structure that oscillates wildly between the limits shown in Fig. 3 although this is allowed for in our bound. To remove this possibility apparently requires an *'a priori'* judgement of reasonable limits on velocity gradients in the Earth and has not been attempted in the present study.

It is clear that we wish to choose the multipliers (the a_is) to minimize contamination, spread and error. This introduces additional tradeoffs between spread and contamination and error and contamination. The tradeoffs can be investigated by adjusting the weightings (λs) in the definition of the spread matrix (equation (4.4)). An obvious strategy is to make

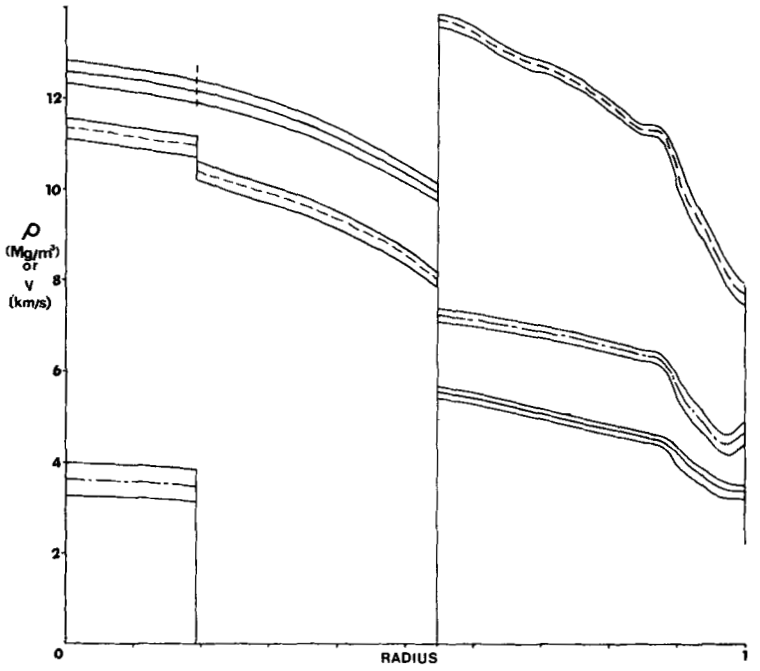

Figure 3. Estimated corridors of possible seismic velocities and density in the Earth: (see Appendix B for references) density (solid line), compression velocity (broken line), shear velocity (chain dotted line).

the λs proportional to the uncertainties in their respective parameters. For example, we believe that the lower mantle compressional velocity of 1066A is very close to that of the real Earth. λ_{v_p} can be made small in this region which means that R_{v_p} is not so well minimized but the contribution to the bound on C_{v_p} will still be small. The absolute values of the λs are then adjusted until a compromise between spread, error and contamination is achieved. More sophisticated definitions of spread can be devised to investigate these tradeoffs, however, (4.4) has proved adequate for this study.

The results of the resolving power analysis are summarized in Fig. 4 and Table 1. The table gives details of the contamination and the resolving kernel R'_η near the knee of the tradeoff curve for each radius, r_0, shown in Fig. 4. The 'centre' of the kernel is defined as the radius from which the spread of the kernel is least. The 'width' of the kernel is the spread about the 'centre'. These quantities may be useful when a disproportionately large contribution to the spread comes from displacement of the peak from r_0 and are defined in Backus & Gilbert (1970).

The total contamination is estimated by:

$$C = [C_{v_p}^2 + C_{v_s}^2 + C_\Delta^2]^{1/2}$$

where the bounds on C_{v_p} etc. have been used. The total uncertainty in the local average is estimated by:

$$\epsilon = [\varepsilon^2 + C^2]^{1/2}.$$

A better idea of the contamination in the answer is given by plots of R_η, R_{v_p} and R_{v_s}. These are shown for selected radii in Figs 5 and 6. For the λs chosen it is clear that contamination is unimportant and this is discussed in Section 6.

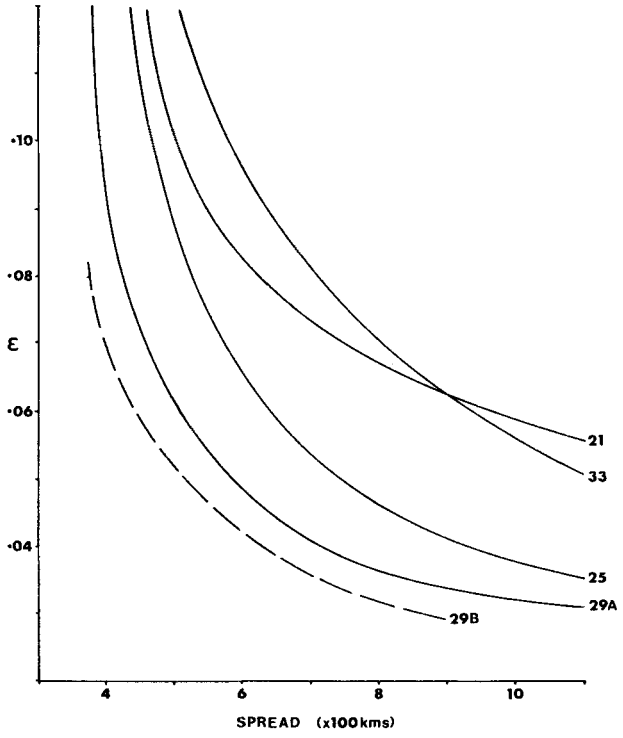

(a)

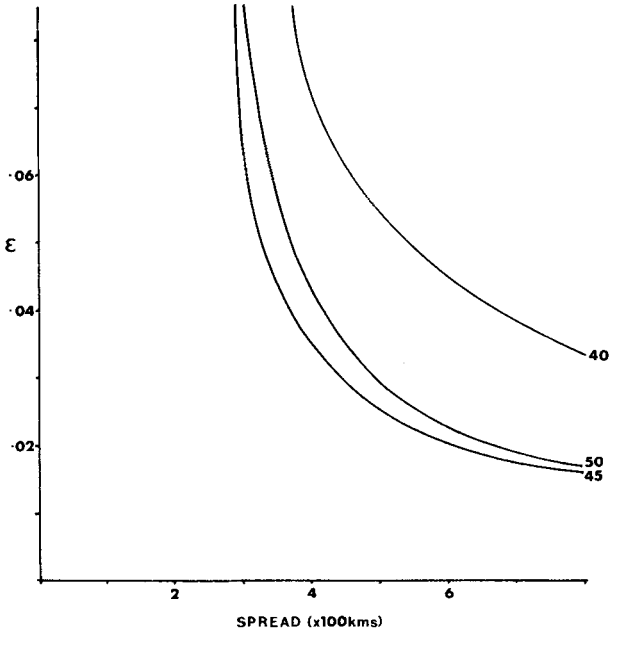

(b)

Figure 4. (a) Tradeoff curves of spread/error for η at various levels in the outer core. The radius of each level is shown in units of 100 km by each curve. (b) Tradeoff curves of spread/error in the lower mantle (see text for explanation).

Table 1

r_o (kms)	centre (kms)	spread (kms)	width (kms)	C_{vp}	C_{vs}	C_Δ	C_{tot}	ε	ϵ	$\bar{\eta}$
2100	2211	733	625	0.002	0.002	0.001	0.003	0.071	0.071	0.998
2500	2523	700	696	0.001	0.002	0.001	0.003	0.053	0.053	1.010
2900	2890	622	621	0.002	0.002	0.002	0.003	0.046	0.046	0.996
3300	3163	712	508	0.003	0.002	0.002	0.004	0.079	0.079	0.976
4000	4128	638	477	0.003	0.002	0.001	0.004	0.042	0.042	1.085
4500	4479	441	436	0.001	0.001	0.001	0.002	0.029	0.029	0.931
5000	4989	500	499	0.003	0.002	0.002	0.004	0.029	0.029	0.931
Boxcar in outer core				0.003	0.003	0.007	0.009	0.050	0.050	0.986

5 Resolvability of the density jump at the ICB

A density jump at the ICB is a feature of all recent earth models although its magnitude is variable from model to model. In this section we determine whether a density jump is required by the modal dataset and, if so, how uncertain is it? 1066A is again used as a reference model. This model has a density jump of 0.87 My m^{-3} which is somewhat larger than most other models and possible reasons for this are discussed below. To determine the uncertainty of the density jump we require an expression relating a perturbation in the density jump to the corresponding perturbation in the eigenfrequency of a mode. The density distribution is considered as a sum of a step function with a step of magnitude Δ

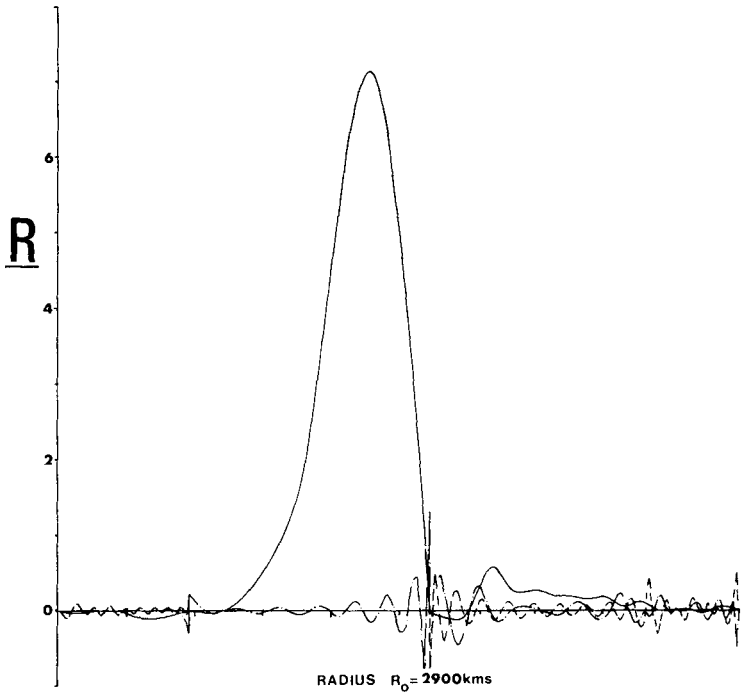

Figure 5. Resolving kernel for radius of 2900 km corresponding to a point near the knee of curve 2900A in Fig. 4(a). Ideally R_{v_p} (chain dotted line) and R_{v_s} (broken line) should be zero while R'_η (solid line) should be peaked at 2900 km. For details see Table 1.

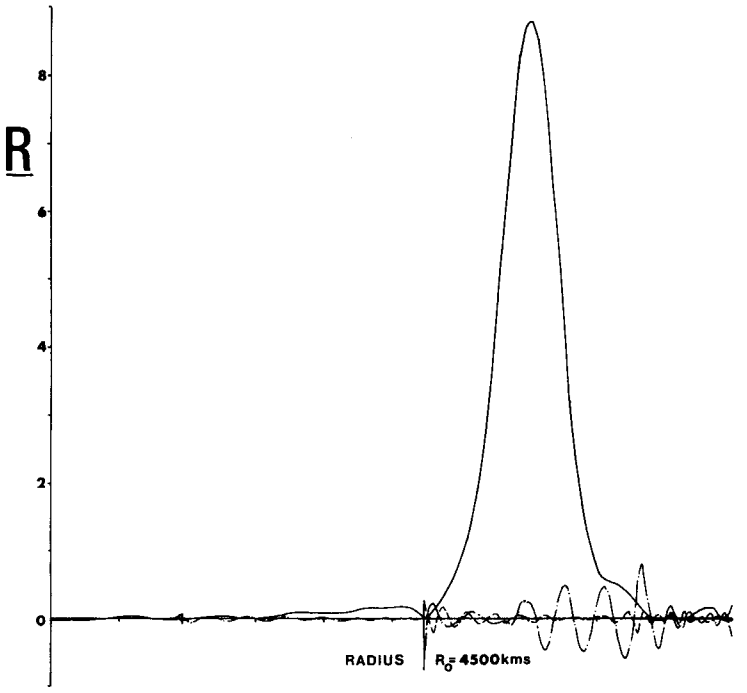

Figure 6. Resolving kernel for a radius of 4500 km. For details see Table 1. Notation as in Fig. 5.

(the density jump at the ICB) and a density distribution ρ_c with a continuous density at the ICB (Fig. 7).

$$\rho = \rho_c + \Delta H(r - r_{\mathrm{ICB}}). \tag{5.1}$$

$H(r - r_{\mathrm{ICB}})$ is the Heaviside step function.

First-order perturbations are related by

$$\frac{\delta\rho}{\rho} = \frac{\rho_c}{\rho}\frac{\delta\rho_c}{\rho_c} + \frac{\delta\Delta H(r - r_{\mathrm{ICB}})}{\rho}. \tag{5.2}$$

Substituting in equation (4.1) we have, for an individual mode:

$$\frac{\delta\omega}{\omega} = \int_0^1 \left(K_{\rho_c}\frac{\delta\rho_c}{\rho_c} + K_{\upsilon_p}\frac{\delta\upsilon_p}{\upsilon_p} + K_{\upsilon_s}\frac{\delta\upsilon_s}{\upsilon_s}\right) r^2\, dr + \delta\Delta A \tag{5.3}$$

$$K_{\rho_c} = \frac{\rho_c}{\rho}K_\rho \qquad A = \int_0^{r_{\mathrm{ICB}}} \frac{K_\rho}{\rho} r^2\, dr.$$

The kernel for the magnitude of the discontinuity, A, is a weighted integral of the density kernel and is not generally sensitive to the position of the discontinuity in the model. This is because K_ρ is simply related to the eigenfunctions of the mode and these are usually smoothly varying. The exception to this is if a mode has a turning point in its wave equation close the to ICB. The nature of the eigenfunctions changes across the turning point and so could affect the value of A if the radius of the ICB is changed. This has been discussed above and may contribute some additional uncertainty to the calculation as those modes which have a variable value of A from model to model have not been excluded from the dataset.

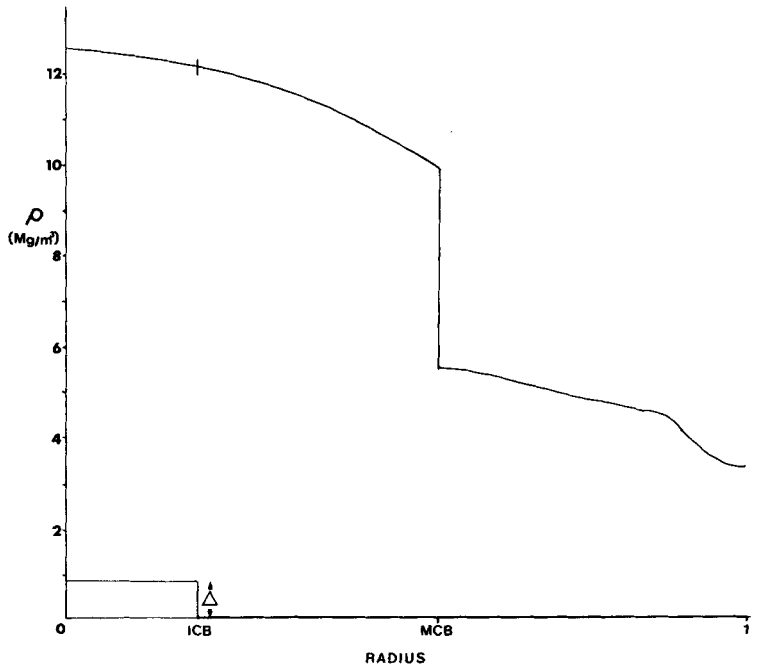

Figure 7. Decomposition of density distribution into 'continuous' and step function parts for calculating the kernels for the density jump at the ICB.

The linearity of changes in the mode frequencies to changes in the size of the density jump alone has been checked. Perturbations in the density jump of 1 Mg m^{-3} give perturbations in the eigenfrequencies of the modes correctly predicted by the kernels and this is larger than any perturbation we expect.

The procedure of the previous section is closely followed. A linear combination of the data kernels is taken:

$$\sum_{i=1}^{m} a_i \left(\frac{\delta\omega}{\omega}\right)_i = \int_0^1 \left(R\rho_c \frac{\delta\rho_i}{\rho_c} + R_{v_p} \frac{\delta v_p}{v_p} + R_{v_s} \frac{\delta v_s}{v_s}\right) r^2 \, dr + \sum_{i=1}^{m} a_i A_i \, \delta\Delta. \tag{5.4}$$

The multipliers are normalized so that

$$\sum_{i=1}^{m} a_i A_i = 1$$

and are chosen to fulfil as best as possible

$$R_{\rho_c} = R_{v_p} = R_{v_s} = 0.$$

A perfect minimization would give

$$\delta\Delta = \sum_{i=1}^{m} a_i \left(\frac{\delta\omega}{\omega}\right)_i. \tag{5.5}$$

The linear combination of residuals is assumed to have its expected value of zero as before.

The contamination in the answer is bounded as in the previous section, i.e.

$$C_{v_p} \leq \int_0^1 |R_{v_p}| \left| \frac{\delta v_p}{v_p} \right|_{\max} dr$$

etc. and the total contamination is estimated by

$$C = [C_{v_p}^2 + C_{v_s}^2 + C_{\rho_c}^2]^{1/2}. \tag{5.6}$$

In this problem there is no 'spread' as such and there is a simple tradeoff between contamination and error where the error is again given by (4.6). Fig. 8 shows the tradeoff curve between contamination and error and gives the details of the contamination at the knee. The total error is estimated by

$$\epsilon = [C^2 + \varepsilon^2]^{1/2}. \tag{5.7}$$

The total error is 0.32 Mg m^{-3} at the knee. The density jump at the inner core boundary is thus 0.87 Mg cm^{-3} ± 0.32 Mg m^{-3}.

An alternative approach is to use the *'a priori'* estimates of the maximum uncertainties in the velocities and densities in a rather more active way (Backus 1970). The following is sometimes called the subjective approach.

The error we make in using the misfit as an estimate of the perturbation in the density jump is

$$\epsilon = \sum_{i=1}^{m} a_i \left(\frac{\delta \omega}{\omega} \right)_i - \delta \Delta = (\mathbf{R}, \mathbf{m}) + \epsilon$$

where

$$\mathbf{R} = R_{\rho_c}, R_{v_p}, R_{v_s} \tag{5.8}$$

and

$$\mathbf{m} = \frac{\delta \rho_c}{\rho_i}, \frac{\delta v_p}{v_p}, \frac{\delta v_s}{v_s}.$$

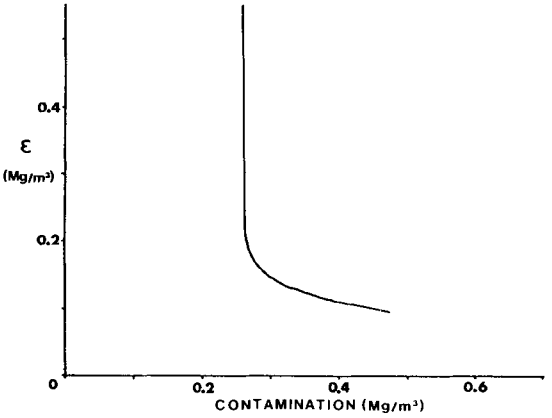

Figure 8. Tradeoff curve of contamination/error for the density jump at the ICB. At the knee: C_{ρ_c} = 0.268 Mg m^{-3}, C_{v_p} = 0.047 Mg m^{-3}, C_{v_s} = 0.012 Mg m^{-3}, C_{TOT} = 0.272 Mg m^{-3}, ε = 0.169 Mg m^{-3}, ϵ = 0.320 Mg m^{-3}, Δ = 0.87 Mg m^{-3} (1066A).

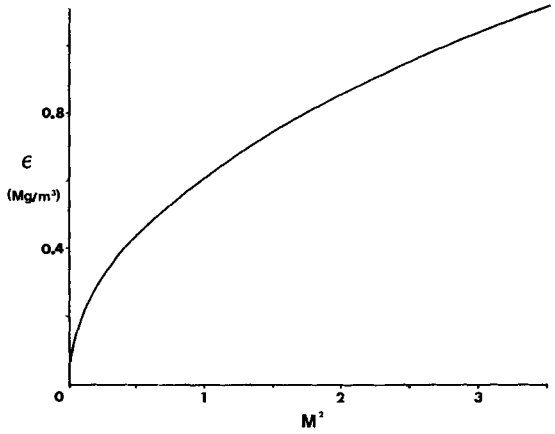

Figure 9. The subjective approach. ϵ is the upper bound on the error on the perturbation to the density jump at the ICB. M is the upper bound on the possible perturbations to the density and seismic velocities of 1066A. $M = 1$ corresponds to the uncertainties shown in Fig. 3.

If the errors in the data have an expected value of zero then

$$\epsilon^2 = (\mathbf{R}, \mathbf{m})^2 + \varepsilon^2.$$

An application of Schwarz inequality gives

$$\epsilon^2 \leqslant (\mathbf{R}, \mathbf{R})\,(\mathbf{m}, \mathbf{m}) + \varepsilon^2.$$

Writing the upper limit chosen for $\mathbf{m}$ as M we have

$$\epsilon^2_{\max} = M^2(\mathbf{R}, \mathbf{R}) + \varepsilon^2. \tag{5.9}$$

The multipliers are chosen to minimize this and now M^2 can be regarded as a tradeoff parameter. Fig. 9 shows ϵ as a function of M^2 where M^2 has been normalized to the uncertainties given in Appendix B. The maximum error given by 5.9 at $M^2 = 1$ is 0.62 Mg m^{-3} which is somewhat larger than before. The use of the Schwarz inequality in this case gives us a pessimistic estimate of the error and this has been found to be so in several applications of this method (Parker 1977).

6 Discussion

The stratification results summarized in Table 1 and Fig. 4 will be discussed first. It is apparent that the λs have been made sufficiently large for the contamination to be unimportant in this calculation. It might be thought that an improvement in spread could be achieved by reducing these weights but this is only done at the expense of a large increase in contamination. This is illustrated in Fig. 4 by the two curves for radius 2900 km. The curve 2900B was produced using weights an order of magnitude smaller than 2900A. The improvement in spread (for a given error) is about 15 per cent but the contamination is increased by a factor of 4. If the total error, ϵ, were plotted against spread for these two curves there would be little to choose between them. It is also apparent from Fig. 4 that the best resolving power is found in the middle of the lower mantle and is relatively poor at the base of this region. In the core the resolving power is best at a radius of ~ 2900 km and falls off towards both boundaries. Jordan & Anderson (1974) found that the resolving power

of a smaller dataset of modes was surprisingly good near the MCB for the individual seismic parameters, v_p, v_s and ρ. This suggests that we should be able to resolve the stratification quite well at the base of the mantle. The reason that we cannot is that we are trying to remove the effect of the density discontinuity and also form a large peak in the resolving kernel near this point. The similarity of the density discontinuity kernels and the kernels in η at the MCB ensure that, to a certain extent, these aims are mutually exclusive (see Appendix A). Good resolution can be achieved if one is prepared to state that the density jump at the MCB is well known. The knees of the tradeoff curves in Fig. 4 are not well defined and to some extent the 'best' point on the tradeoff curve is a matter of personal choice. Because small-scale variations in the stratification parameter are not expected, except near discontinuities, I have chosen to tabulate comparatively large spread solutions. In the core these are still accompanied by comparatively large errors. These errors are too large to allow us to exclude a thermally stratified core of the type proposed by Higgins & Kennedy (1971) over any resolving length. The local averages over the model are not significantly different from unity in this region. This result depends upon the assumption that 1066A is linearly close to the real Earth and this should be checked before any reliance can be placed on this answer. A simple way to do this would be to repeat the analysis with a different reference model. If the 'corrected' local averages were consistent with those given above then this would considerably reinforce the credibility of the answers. This calculation would be somewhat lengthy and limited inferences can be made from numerical experiments which do suggest that non-linearity is unimportant. For example, perturbations of several per cent have been found to be within the range of linearity but to a certain extent this depends upon the nature of the perturbation and the particular mode being tested. The remaining difficulty of possible systematic error in the dataset will be easier to assess with the accumulation of more data.

The large errors associated with the relatively large spreads in the core indicates that the detail shown in the stratification parameter in most modern earth models is inappropriate. For this reason a calculation was performed to see if a reasonably accurate average value of η for the whole outer core could be obtained. The appropriate shape for the resolving kernel in this case is a boxcar and an attempt at making such a kernel is shown in Fig. 10. The details of results of this calculation are shown in Table 1. The results suggest that the average value of η is close to unity and has an uncertainty of 0.05. This is sufficiently small to allow us to exclude the possibility of a strongly chemically stratified core of the type proposed by Usselman (1975), i.e. where the chemical stratification occurs over the whole outer core.

The resolving power of the data in the lower mantle is better than in the core. The results show the somewhat disturbing feature of a significantly stable region in the lower 1000 km. The apparent stability is too great for any subadiabatic temperature gradient and implies a chemical stratification of the lower mantle. Again we rely on the linearity assumption and this should be checked using another reference model. It is interesting to note that, in Fig. 1, both 1066A and B are stable on average in the middle of the lower mantle. Also, all three models show a tendency to go unstable towards the MCB. This seems to favour the interpretation of the D″ region in terms of a thermal boundary layer although the evidence is far from compelling.

The calculation of the uncertainties on the density jump at the ICB is more satisfactory. The results suggest that the density jump is greater than 0.3 Mg m^{-3} even if the observational errors on the modes are doubled. This value is significantly larger than the density jumps in models C-2 and B1 of Anderson & Hart (1976) and Jordan & Anderson (1974) even if the observational errors on the modes are doubled. A possible explanation is that many of the modes sensitive to the density jump at the ICB are not used by these workers in their

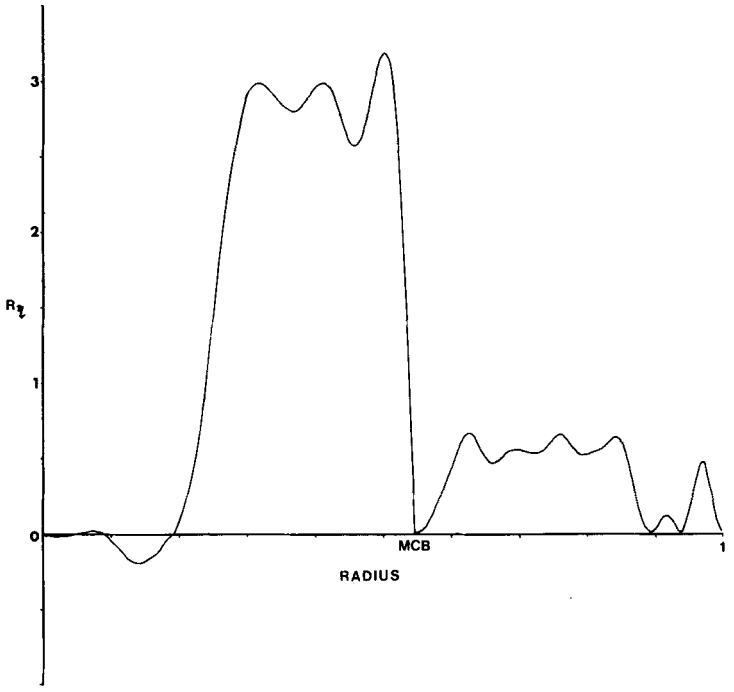

Figure 10. An attempt to make a boxcar-like resolving kernel in the outer core. For details of contamination, etc., see Table 1.

inversions as they limit the number of spheroidal overtones to reduce computational labour. This hypothesis is supported by a consideration of the starting models used to construct 1066A and B. Model 508 has a density jump of 1.08 Mg m^{-3} which was reduced to 0.87 Mg m^{-3} when iterated to 1066A using the full dataset. Model B1 has a density jump of 0.17 Mg m^{-3} which was increased to 0.56 Mg m^{-3} when iterated to 1066B. Care must be taken when interpreting these trends as there are tradeoffs with inner core radius and shear velocity but a density jump of 0.7 Mg m^{-3} seems to be indicated with an uncertainty of 0.3–0.4 Mg m^{-3}. The significance of these results for the thermal and chemical state of the core and lower mantle are discussed in the next section.

7 Conclusions

A common explanation for the existence of the inner core is to consider it as an evolutionary feature of a cooling earth (Verhoogen 1961). The outer core is thought to be mainly composed of iron with some light elements (sulphur or silicon are strong contenders for the main impurity). Metallurgical experience suggests that, if the core cools slowly, iron and heavier metals will solidify out and will reject most of the lighter constituents at the boundary between solid and liquid. This mechanism leaves an excess of light material near the ICB which will be gravitationally buoyant. Gubbins (1977), developing an idea of Braginsky (1964), has shown that the loss of gravitational energy caused by the mixing of this light element can be efficiently converted into magnetic energy and therefore the existence of a compositional difference between the inner and outer cores could be indicative of a power source for the geodynamo. If the inner core is pure iron, shock wave data suggest that the density jump at the ICB will be approximately 1 Mg m^{-3} (Al'tschuler,

Simakov & Trunin 1968). Such a density jump can be accommodated by the free oscillation data. If the inner and outer cores were of the same composition and the density difference simply due to solidification, the gravitational power source would be removed. The density jump due to solidification can be estimated using the Clapeyron equation and the assumption of hydrostatic equilibrium:

$$\Delta = -\frac{\rho L}{g}\frac{d \ln T_m}{dr} \tag{7.1}$$

where L is the latent heat of solidification of core material and T_m is the melting temperature. $d \ln T_m/dr$ has been estimated for pure iron by many people and changes little from study to study even though T_m varies considerably. The addition of impurities reduces both dT_m/dr and T_m and so we can use the estimate of $d \ln T_m/dr$ for iron without much error. Using Verhoogen's (1961) estimate of L we have $\Delta \simeq 0.05$ Mg m^{-3}. This is much smaller than the minimum density jump demanded by the data and we can conclude that a compositional difference is required by the data. This point is discussed in more detail in Gubbins *et al.* (in preparation).

It is more difficult to extract strong conclusions from the stratification results. The possibility of a stable region near the surface of the core such as could be due to an accumulation of light material released by the growth of the inner core cannot be excluded. The data allow plenty of room for speculation. The core is apparently not stratified near the inner core boundary and this conclusion is strengthened by the increased sensitivity of η to chemical gradients in this region (Section 2). The results in the lower mantle are also of interest and it remains to be seen if the apparent stability of this region is real. On the basis of the models shown in Fig. 1 it is apparent that the data support neither of the extreme values of η proposed in Section 2 for the base of the mantle. While it could be argued that the modal data are unable to resolve the structure in this relatively small region of at most 200 km, the models do seem to favour a thermal boundary layer interpretation. A further difficulty with the use of the normal mode dataset arises because of the first-order effects of attenuative dispersion on model structures. This has been demonstrated in a recent series of papers (see Kanamori & Anderson 1977 for a review) and has the effect of making the seismic parameters frequency-dependent. A model constructed at a reference frequency of 1 s (Hart, Anderson & Kanamori 1977) showed that changes in structure from models which ignored this effect were largest in regions of low Q or high attenuation. Because the attenuation is small in the lower mantle and outer core (according to Cormier & Richards (1976), Q is practically infinite in the outer core); this should have little effect on the conclusions drawn here. The possibility of a low Q zone at the base of the mantle might affect some of the calculations but presumably reinforces the interpretation of the base of the mantle as a thermal boundary layer.

The expansion and improvement of the present modal dataset is now being undertaken through Project IDA. This will eliminate many of the difficulties encountered in the preceding sections and will also improve the resolving power of the dataset. Further techniques can also be applied to improve the resolving power and the fact that $\eta \geqslant 1$ in much of the deep Earth should prove a useful constraint in this respect. The formulation of the inverse problem for the normal modes in terms of η, v_p, v_s instead of ρ, v_p, v_s also has some intrinsic advantages. In particular this allows easy incorporation of constraints on stratification and tends to result in smoother earth models.

In conclusion the results of this investigation, although subject to some uncertainty, suggest that in the near future the modal dataset will be able to provide useful constraints on the chemical and thermal structure of the deep Earth.

Acknowledgments

David Gubbins has contributed a great deal to this paper, particularly in the analysis of Appendix A. He and Jack Jacobs have critically read the manuscript and many of their suggestions have been adopted. Part of this work was performed during a visit to Boulder, Colorado and La Jolla, San Diego. I wish to acknowledge support from grants: NSF DES75-03237 and NASA NSG7319. Many thanks to Martin L. Smith for organizing this and to everybody who made my visit so profitable. In particular, Freeman Gilbert and Ray Buland provided many of their progams for my use and contributed many useful comments. This work was performed during the tenure of a NERC studentship.

References

Al'tschuler, L. V., Simakov, G. V. & Trunin, R. F., 1968. On the composition of the Earth's core, *Isv. Earth Phys.*, **1**.

Anderson, D. L. & Hart, R. S., 1976. An Earth model based on free oscillations and body waves, *J. geophys. Res.*, **81**, 1461.

Backus, G. E., 1970. Inference from inadequate and inaccurate data I, *Proc. Nat. Acad. Sci. U.S.A.*, **65**, 1.

Backus, G. E. & Gilbert, J. F., 1967. Numerical applications of a formulation for geophysical inverse problems, *Geophys. J.*, **13**, 247.

Backus, G. E. & Gilbert, J. F., 1968. The resolving power of gross Earth data, *Geophys. J.*, **16**, 169.

Backus, G. E. & Gilbert, J. F., 1970. Uniqueness in the inversion of inaccurate gross Earth data, *Phil. Trans. R. Soc. Lond. A*, **266**, 123.

Berger, J., Agnew, D. & Farrell, W. E., 1975. A worldwide network of very long period seismometers, *EOS*, **55**, 1024.

Birch, F., 1952. Elasticity and constitution of the Earth's interior, *J. geophys. Res.*, **57**, 227.

Bolt, B. A., 1972. The density distribution near the base of the mantle and near the Earth's centre, *Phys. Earth planet. Int.*, **5**, 301.

Braginsky, S. I., 1964. Magnetohydrodynamics of the Earth's core, *Geomag. Aeron.*, **4**, 572.

Bullen, K. E., 1963. An index of degree of chemical inhomogeneity in the Earth, *Geophys. J.*, **7**, 584.

Bullen, K. E., 1967. Note on the coefficient η, *Geophys. J.*, **13**, 459.

Bullen, K. E., 1975. *The Earth's Density*, Chapman & Hall, London.

Busse, F. H., 1975. A model of the geodynamo, *Geophys. J.*, **42**, 437.

Chandrasekhar, S., 1961. *Hydrodynamic and Hydromagnetic Stability*, Clarendon Press, Oxford.

Choy, G. L., 1977. Theoretical seismograms of core phases calculated by frequency dependent full wave theory, and their interpretation, *Geophys. J.*, **51**, 275.

Cleary, J. R., 1974. The D″ region, *Phys. Earth planet. Int.*, **9**, 13.

Cormier, V. F. & Richards, P. G., 1976. Comments on "The damping of core waves" by A. Qamar and A. Eisenberg, *J. geophys. Res.*, **81**, 3066.

Dziewonski, A. M. & Gilbert, J. F., 1973. Observations of normal modes from 84 readings of the Alaskan earthquake of 1964 March 18 II, *Geophys. J.*, **35**, 401.

Dziewonski, A. M., Hales, A. L. & Lapwood, E. R., 1975. Parametrically simple earth models consistent with Geophysical data, *Phys. Earth planet. Int.*, **10**, 12.

Gilbert, J. F., 1971. Ranking and winnowing of gross Earth data, *Geophys. J.*, **23**, 125.

Gilbert, J. F. & Dziewonski, A. M., 1975. An application of normal mode theory to the retrieval of structural parameters and source mechanisms from seismic spectra, *Phil. Trans. R. Soc. Lond. A*, **278**, 187.

Goldreich, P. & Toomre, A., 1969. Some remarks on polar wandering, *J. geophys. Res.*, **74**, 2555.

Gubbins, D., 1976. Observational constraints on the generation process of the Earth's magnetic field, *Geophys. J.*, **47**, 19.

Gubbins, D., 1977. Energetics of the Earth's core, *J. Geophys.*, **43**, 453.

Hart, R. S., Anderson, D. L. & Kanamori, H., 1977. The effect of attenuation on gross earth models, *J. geophys. Res.*, **82**, 1647.

Higgins, G. & Kennedy, G. C., 1971. The adiabatic gradient and the melting point gradient in the core of the Earth, *J. geophys. Res.*, **72**, 1370.

Jacobs, J. A., 1975. *The Earth's Core*, Academic Press, London.

Johnson, L. E. & Gilbert, J. F., 1972. Inversion and inference for teleseismic ray data, in *Methods in Computational Physics*, vol. 12, Academic Press, London.

Jones, G. M., 1977. Thermal interaction of the core and the mantle and long term behaviour of the geomagnetic field, *J. geophys. Res.*, **82**, 1703.

Jordan, T. M. & Anderson, D. L., 1974. Earth structure from free oscillations and travel times, *Geophys. J.*, **36**, 411.

Kanamori, H. & Anderson, D. L., 1977. Importance of physical dispersion in surface wave and free oscillation problems: review, *Rev. Geophys. Space. Phys.*, **15**, 105.

Massé, R. P., Flinn, E. A., Seggelke, R. M. & Engdahl, E. R., 1976. PKIIKP and the average velocity of the inner core, *Geophys. Res. Lett.*, **1**, 39.

Mckenzie, D. P., 1966. The viscosity of the lower mantle, *J. geophys. Res.*, **71**, 3995.

Mckenzie, D. P., Roberts, J. M. & Weiss, N. O., 1974. Convection in the Earth's mantle: towards a numerical simulation, *J. Fluid. Mech.*, **62**, 465.

Parker, R. L., 1977. Linear inference and underparameterised models, *Rev. Geophys. Space. Phys.*, **15**, 446.

Pekeris, C. L. & Accad, Y., 1972. Dynamics of the liquid core of the Earth, *Phil. Trans. R. Soc. Lond. A*, **273**, 237.

Piaggio, H. T. H., 1958. *Differential Equations*, Bell & Sons Ltd, London.

Press, F., 1972. The Earth's interior as inferred from a family of models, in *The Nature of the Solid Earth*, ed. Robertson, McGraw-Hill.

Tozer, D. C., 1972. The present thermal state of the terrestrial planets, *Phys. Earth planet. Int.*, **6**, 182.

Usselman, T. M., 1975. Experimental approach to the state of the core II. Composition and thermal regime, *Am. J. Soc.*, **275**, 291.

Verhoogen, J., 1961. Heat balance of the Earth's core, *Geophys. J.*, **4**, 276.

Wiggins, R. A., McMechan, G. A. & Tokzov, M. N., 1973. Range of Earth structure nonuniqueness implied by body wave observation, *Rev. Geophys. Space Phys.*, **11**, 87.

Woodhouse, J. H., 1976. On Rayleigh's principle, *Geophys. J.*, **46**, 11.

Appendix A: kernels for the stratification parameter η

Our starting point for the derivation of the kernels is equation (49) of Backus & Gilbert (1967) which is simply rewritten to give:

$$\frac{\delta\omega}{\omega} = \int_0^1 \left(K_{v_p} \frac{\delta v_p}{v_p} + K_{v_s} \frac{\delta v_s}{v_s} + K_\rho \frac{\delta\rho}{\rho} \right) r^2 \, dr. \tag{A1}$$

The radius has been normalized to the surface value. This equation relates the perturbations in seismic velocities and densities to the perturbation in the eigenfrequency of an individual mode. The kernels K_{v_p}, K_{v_s} and K_ρ are simple functions of the eigenfunctions of the mode and so can be calculated for a particular earth model. The stratification parameter is defined by equation (1.3)

$$\eta = -\frac{\phi}{\rho g}\frac{d\rho}{dr}.$$

First-order relative perturbations are therefore given by:

$$\frac{\delta\eta}{\eta} = \frac{\delta\phi}{\phi} + \frac{\delta\rho'}{\rho'} - \frac{\delta\rho}{\rho} - \frac{\delta g}{g}$$

where the prime denotes the radial gradient. At a density discontinuity η is singular. Because of this, the notation $\int$ is used to designate integration over intervals between discontinuities and not through them.

Suppose K is the required kernel for the perturbation in stratification, then:

$$\oint_0^1 Kr^2\left(\frac{\delta\eta}{\eta}-\frac{\delta\phi}{\phi}\right)dr=\oint_0^1 K\left(\frac{\delta\rho'}{\rho'}-\frac{\delta\rho}{\rho}-\frac{\delta g}{g}\right)r^2\,dr. \tag{A2}$$

Integrating by parts gives

$$\oint_0^1 K\frac{\delta\rho'}{\rho'}r^2\,dr=\sum_{i=1}^{m}\left[\frac{\rho Kr^2}{\rho'}\frac{\delta\rho}{\rho}\right]_{i+\epsilon}^{i+1-\epsilon}-\oint_0^1\left(\frac{Kr^2}{\rho'}\right)'\frac{\rho}{r^2}\frac{\delta\rho}{\rho}r^2\,dr. \tag{A3}$$

The index i denotes the ith discontinuity, the summation sign indicating that there are m intervals between discontinuities. We also have

$$\oint_0^1\frac{K}{g}\delta g r^2\,dr=-\oint_0^1 L4\pi G\rho\frac{\delta\rho}{\rho}r^2\,dr+\sum_{i=1}^{m}[L\delta g r^2]_{i+\epsilon}^{i+1-\epsilon}$$

where

$$L=\int\frac{K}{g}dr.$$

Noting that

$$[L\delta g r^2]_{i+\epsilon}^{i+1-\epsilon}=L_{i+1-\epsilon}\int_0^{r_{i+1}}4\pi G\rho\frac{\delta\rho}{\rho}r^2\,dr-L_{i+\epsilon}\int_0^{r_i}4\pi G\rho\frac{\delta\rho}{\rho}r^2\,dr$$

we have

$$\sum_{i=1}^{m}[L\delta g r^2]_{i+\epsilon}^{i+1-\epsilon}=-\sum_{i=1}^{m-1}[L]_i\int_0^{r_i}4\pi G\rho\frac{\delta\rho}{\rho}r^2\,dr+L(1)\int_0^1 4\pi G\rho\frac{\delta\rho}{\rho}r^2\,dr$$

where $[L]_i$ denotes the jump in L at the ith discontinuity and $L(1)$ is the surface value of L. K is proportional to ρ' so L is discontinuous at internal boundaries. To simplify the algebra and the computation we consider L as the sum of continuous and discontinuous parts:

$$L(r)=L_c(r)+[L_i]H(r_i-r)$$

where

$$H(r_i-r)=0\quad r<r_i$$

$$H(r_i-r)=1\quad r>r_i.$$

Then we have

$$\oint_0^1\frac{K}{g}\delta g r^2\,dr=\sum_{i=1}^{m}\left[-[L]_i\int_{r_i}^1 4\pi G\frac{\delta\rho}{\rho}\rho r^2\,dr-[L]_i\int_0^{r_i}4\pi G\rho\frac{\delta\rho}{\rho}r^2\,dr\right]$$
$$-\int_0^1 4\pi GL_c\rho\frac{\delta\rho}{\rho}r^2\,dr+L(1)\int_0^1 4\pi G\rho\frac{\delta\rho}{\rho}r^2\,dr.$$

Using

$$L(1) = L_c(1) + \sum_{i=1}^{m-1} [L]_i$$

the expression simplifies to:

$$\oint_0^1 \frac{K}{g} \delta g r^2 \, dr = - \int_0^1 4\pi G\rho [L_c - L_c(1)] \frac{\delta\rho}{\rho} r^2 \, dr. \tag{A4}$$

Substituting (A4) and (A3) into (A2) gives

$$\oint_0^1 K \left(\frac{\delta\eta}{\eta} - \frac{\delta\phi}{\phi}\right) r^2 \, dr = \oint_0^1 \left[4\pi G\rho(L_c - L_c(1)) - K - \frac{\rho}{r^2}\left(\frac{Kr^2}{\rho'}\right)'\right] \frac{\delta\rho}{\rho} r^2 \, dr.$$

We now make the identification

$$K_\rho = 4\pi G\rho [L_c - L_c(1)] - K - \frac{\rho}{r^2}\left(\frac{Kr^2}{\rho'}\right)'$$

or

$$K = -\frac{\rho'}{\rho r^2} \int_0^r [4\pi G\rho(L_c - L_c(1)) - K_\rho] r^2 \, dr \tag{A5}$$

and

$$L_c = \int_{\text{cont}} \frac{K}{g} \, dr \tag{A6}$$

where the $\int_{\text{cont}}$ is continuous across discontinuities. The solution of (A5), (A6) is discussed below. The identification gives

$$\oint_0^1 K \left(\frac{\delta\eta}{\eta} - \frac{\delta\phi}{\phi}\right) r^2 \, dr = \int_0^1 K_\rho \frac{\delta\rho}{\rho} r^2 \, dr + \sum_{i=1}^{m} \left[\frac{Kr^2\rho}{\rho'} \frac{\delta\rho}{\rho}\right]_{i+\epsilon}^{i+1-\epsilon}.$$

(A5) ensures that $Kr^2\rho/\rho'$ is continuous across a discontinuity. We can also write $\delta\phi/\phi$ in terms of the perturbations to the seismic velocities:

$$\frac{\delta\phi}{\phi} = \frac{2}{1-x} \frac{\delta v_p}{v_p} - \frac{2x}{1-x} \frac{\delta v_s}{v_s}$$

where

$$x = \frac{4}{3} \frac{v_s^2}{v_p^2}$$

$$\therefore \int_0^1 K_\rho \frac{\delta\rho}{\rho} r^2 \, dr = \oint_0^1 \left(K \frac{\delta\eta}{\eta} - \frac{2K}{(1-x)} \frac{\delta v_p}{v_p} + \frac{2Kx}{(1-x)} \frac{\delta v_s}{v_s}\right) r^2 \, dr + \sum_{i=1}^{m-1} \left[\frac{Kr^2\rho}{\rho'}\right]_i \left[\frac{\delta\rho}{\rho}\right]_i$$

$$- \left[\frac{\rho K}{\rho'}\right]_1 \left[\frac{\delta\rho}{\rho}\right]_1.$$

Substitution into (A1) gives

$$\frac{\delta\omega}{\omega} = \int_0^1 \left[\kappa_\eta \frac{\delta\eta}{\eta} + \kappa_{v_p} \frac{\delta v_p}{v_p} + \kappa_{v_s} \frac{\delta v_s}{v_s}\right] dr + \sum_{j=1}^{m} A_j \left[\frac{\delta\rho}{\rho}\right]_j \tag{A7}$$

where

$$\kappa_\eta = Kr^2$$

$$\kappa_{v_p} = \left(K_{v_p} - \frac{2K}{1-x}\right) r^2$$

$$\kappa_{v_s} = \left(K_{v_s} + \frac{2Kx}{1-x}\right) r^2$$

$$A_j = \left[\frac{Kr^2\rho}{\rho'}\right] \quad j \neq m$$

$$A_m = -\left[\frac{\rho K}{\rho'}\right]_1.$$

Once K is determined we can calculate all the kernels in equation (A7). There is an apparent difficulty with the solution of (A5), (A6) as (A6) suggests the possibility that L_c may be infinite at the centre of the Earth ($g = 0$). This difficulty does not arise. To see this we note first that both g and ρ' are proportional to r near the centre. If $L_c(0)$ is finite then (A5) shows that $K \propto r^2$ near the origin so giving $L_c \propto r^2$. Suppose now that $L_c(0)$ is infinite and is proportional to r^{-n} where n is a positive number. (A5) then gives $K \propto r^{-n+2}$ which also gives $L_c \propto r^{-n+2}$. This contradicts our supposition and we can conclude that both L_c and $K \to 0$ as $r \to 0$.

(A5) is an integral equation for K and can be solved in a variety of ways. Perhaps the simplest way is an application of Picards' method using

$$K = \frac{\rho'}{\rho r^2} \int_0^r K_\rho r^2 \, dr \tag{A8}$$

as an initial solution. This iterative procedure ensures that all the boundary conditions are satisfied and convergence is guaranteed (Piaggio 1958, chapter 10). (A8) is usually a good approximation to the solution so convergence is rapid.

Appendix B

The results of Section 4 indicate that our ability to resolve stratification in the Earth is relatively insensitive to the contamination and consequently to the assumed uncertainties in the seismic parameters. This is not true, however, of the density jump at the ICB which is more difficult to isolate from the data. For this reason a discussion of the uncertainties summarized by Fig. 3 seems appropriate. The work of Wiggins, McMechan & Tokzov (1973) gives a clear idea of the uncertainties in the velocity structure below 200 km depth as given by travel-time data. The P velocity in the inner and outer core is uncertain by 2 per cent except for the top-most 100 km of the core where a larger uncertainty is indicated. This is due to the possibility of a low P velocity just below the MCB. Such a possibility has been shown to be unlikely by the work of Choy (1977) so a 2 per cent uncertainty is used throughout the whole core. This may be pessimistic, for example Massé *et al.* (1976) report

a single detection of the phase PKIIKP which, they claim, constrains the compressional velocity in the outer part of the inner core to 0.5 per cent. The shear wave velocity in the inner core is taken to be uncertain by 10 per cent. This is probably generous as the shear velocity is tightly constrained by the observation of an inner core mode (Dziewonski & Gilbert 1973). In the lower mantle (between the core–mantle boundary and the 670 km discontinuity), the P velocity is known to about 1 per cent and the shear velocity to about 1.5 per cent. The uncertainty increases in both velocity distributions towards the upper boundary. Above 700 km depth the P velocity is uncertain by about 3.5 per cent. The shear velocity is apparently uncertain by about 7 per cent in between the 400 and the 670 km discontinuities and by 3 per cent above this.

Wiggins *et al.* claims that restricting the depths of the discontinuities in S to be the same as those of P will considerably tighten these bounds. For simplicity I have chosen an average uncertainty of 5 per cent in v_s above 670 km. Tighter bounds are probably unjustified particularly as we are concerned with a spherically averaged earth model which may be very different from the real Earth in the top few hundred kilometres. The velocities in the 'average' crust are assumed known to 10 per cent.

The uncertainty in density of the lower mantle and core is estimated from the work of Press (1972). Press quotes a band of about 0.3 Mg m^{-3} in the outer core and 0.25 Mg m^{-3} in the lower mantle corresponding to maximum perturbations in density of about 1.5 and 2.5 per cent respectively. The inner core density is as uncertain as the density jump at the inner core boundary which is one of the parameters we are trying to infer. The 'continuous' density distribution in the inner core will have about the same uncertainty as the density in the outer core. The uncertainty in the density distribution in the upper mantle has been obtained by plotting a number of recent earth models and drawing an envelope around the solutions. Although the models are very similar an uncertainty of 0.3 Mg m^{-3} seems appropriate which is consistent with the bands of models presented by Press; this gives an uncertainty of 5 per cent in this region. In the stratification problem an estimate of $[\delta\rho/\rho]^+_-$ is required which is the difference in perturbations in density on either side of a discontinuity. This is difficult to estimate in the upper mantle because of the fact that we have modelled what are probably second-order discontinuities by first order jumps. In 1066A no density jumps are introduced in the upper mantle but different models have jumps of up to 0.3 Mg m^{-3}. This gives $[\delta\rho/\rho]^+_{-\max}$ about 6–7 per cent for the upper mantle jumps. The same value was taken for the jump at the MCB although this is probably generous.

In conclusion, it should be noted that the corridors of possible velocity and density distribution derived from these considerations include all recent earth models.